

**Supporting Information for
Nanoscale Engineering of Porous Fe-doped Pd Nanosheets
Assemblies for Efficient Methanol and Ethanol Electrocatalysis**

Hui Xu, Hongyuan Shang, Cheng Wang, Liujun Jin, Chunyan Chen and Yukou Du *

*College of Chemistry, Chemical Engineering and Materials Science, Soochow
University, Suzhou 215123, PR China*

* Corresponding author: Tel: 86-512-65880967, Fax: 86-512-65880089;
E-mail: duyk@suda.edu.cn (Y. Du)

The electrochemically active surface area (ECSA) of the catalysts can be calculated by integrating the reduction peaks of Pd oxides *via* the equation: $ECSA = Q/(0.43 \times m)$, where Q (mC) is the reduction charge of Pd oxides, 0.43 (mC cm⁻²) is a constant assuming that a monolayer of Pd oxides is reduced on the Pd surface and m (mg) is the mass of Pd loading on the surface of working electrode.

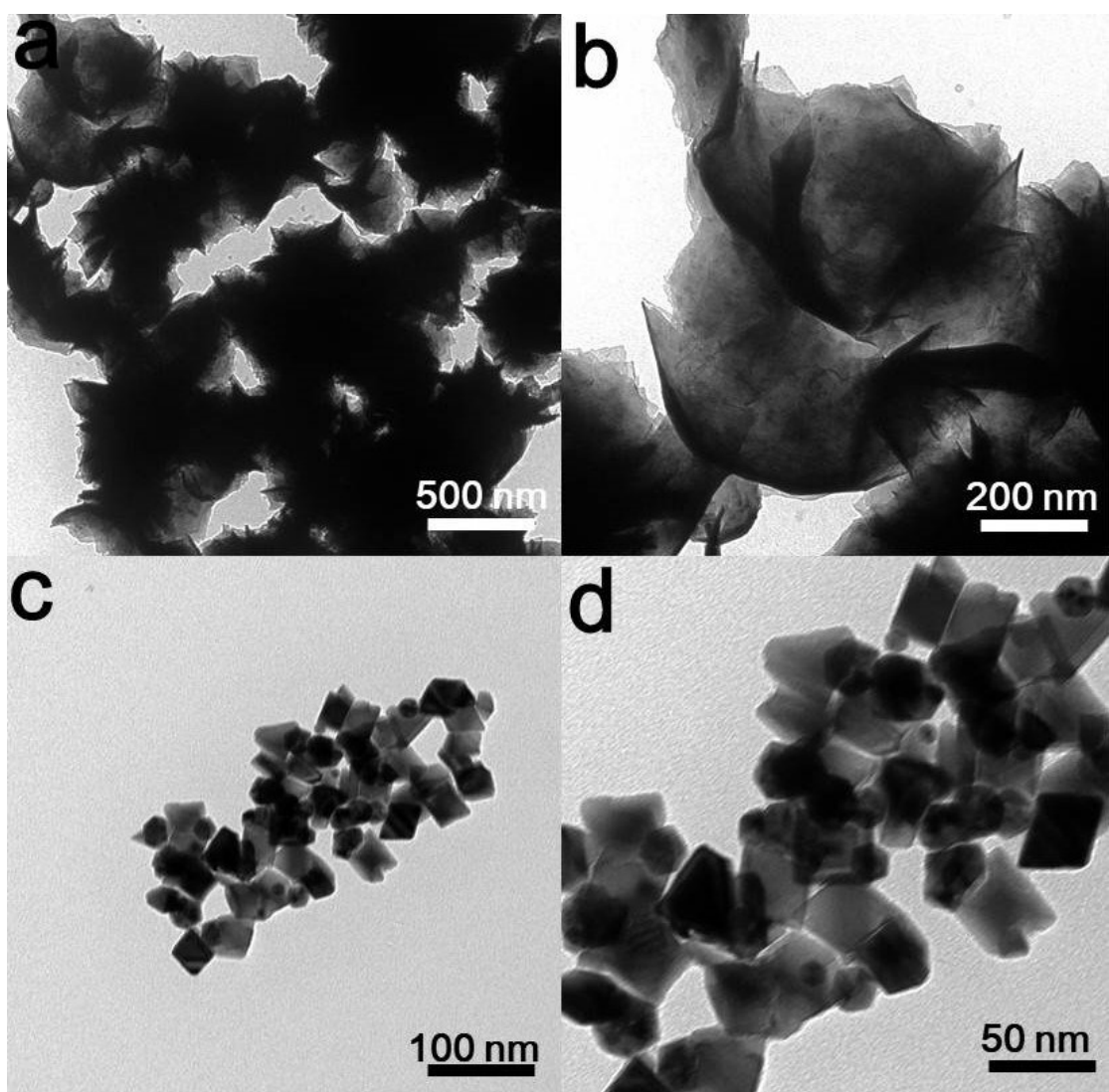


Fig.S1 TEM images of PdFe nanocrystals prepared without the addition of (a and b) PVP and (c and d) $\text{W}(\text{CO})_6$ with different magnifications.

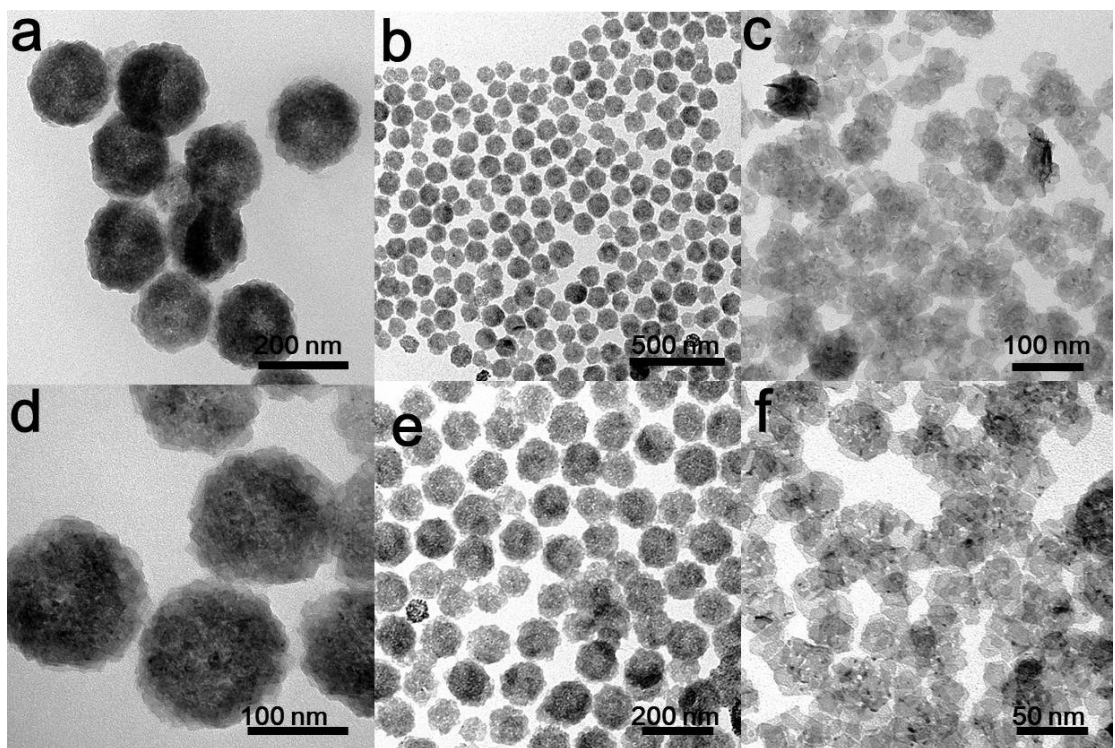


Fig.S2 Additional TEM images of (a and d) PdFe HNSs, (b and e) PdFe NCs, and (c and f) PdFe NPs with different magnifications.

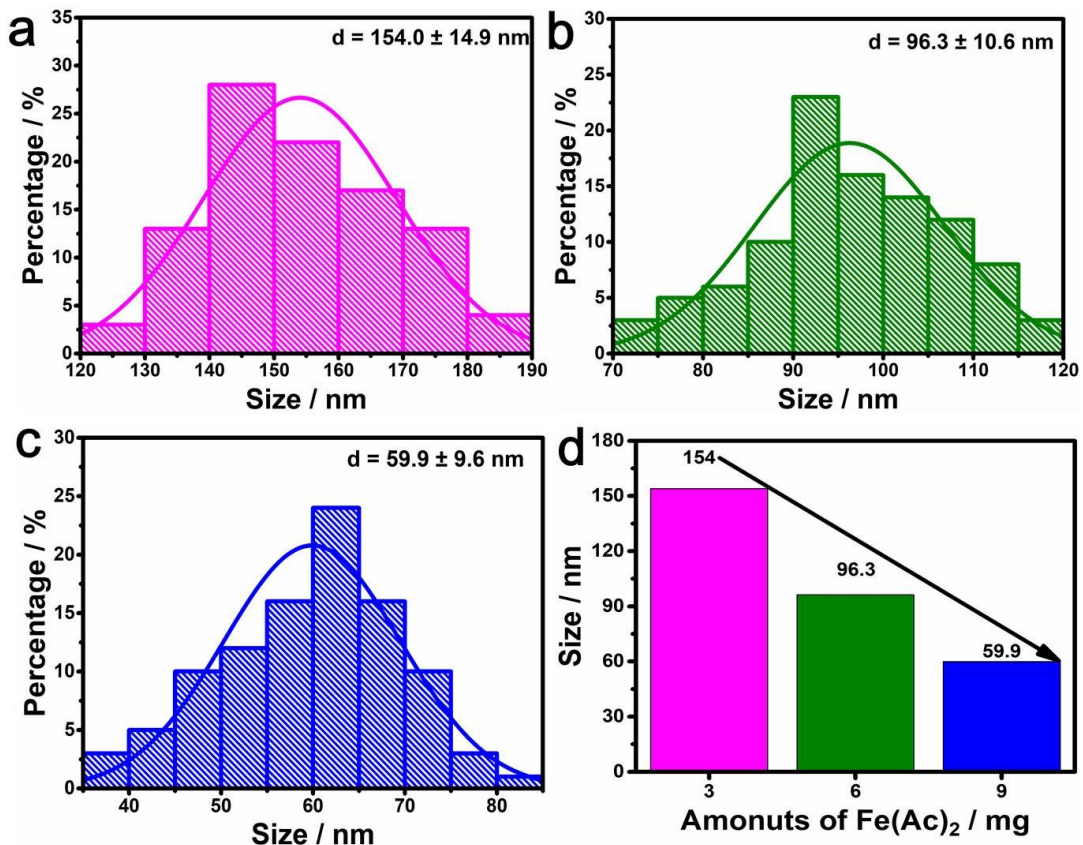


Fig.S3 Histograms for the diameter distribution of (a) PdFe HNSs, (b) PdFe NCs, and (c) PdFe NPs. (d) The comparison histograms of PdFe nanocrystals with the different amounts of $\text{Fe}(\text{Ac})_2$.

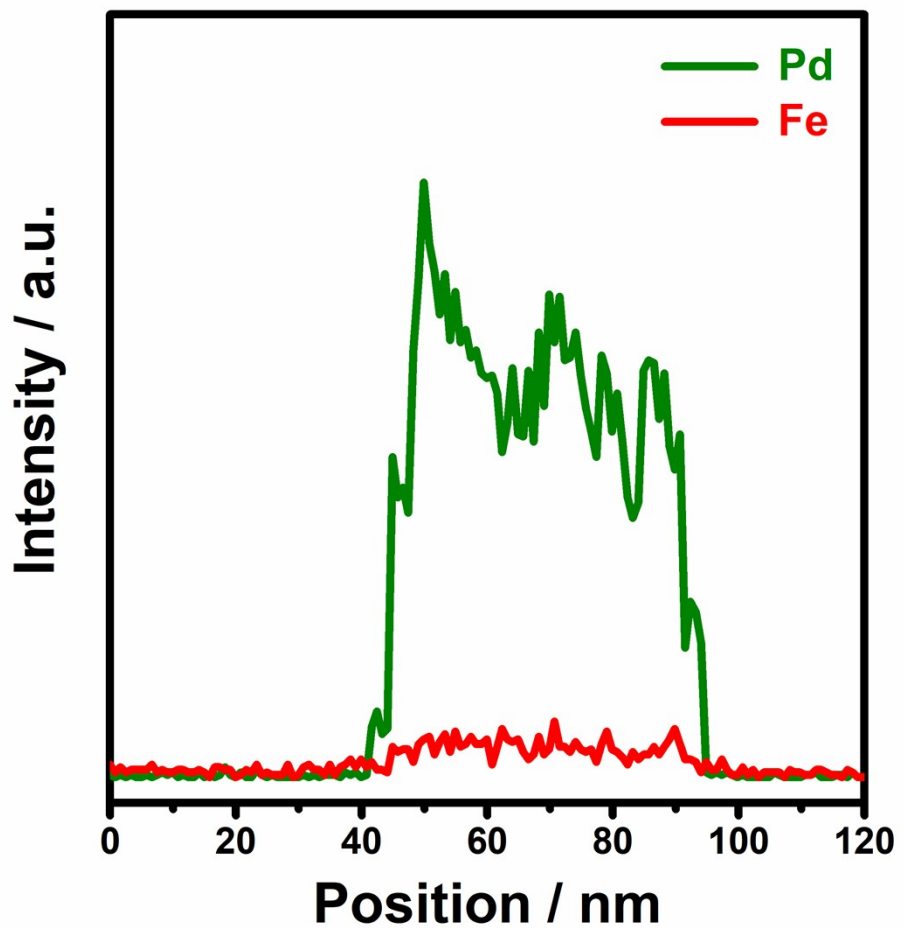


Fig.S4 The line scans of PdFe hollow nanospheres.

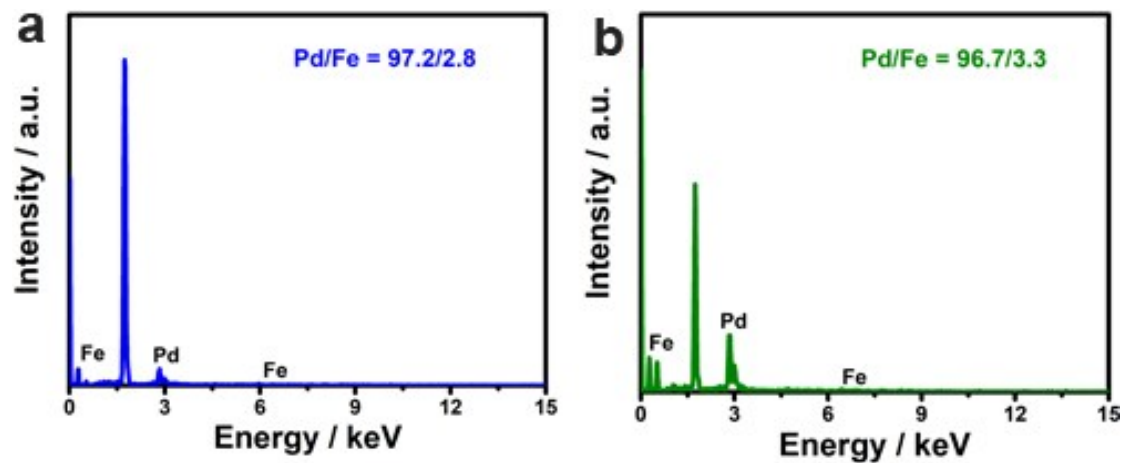


Fig.S5 EDX spectrum of (a) PdFe HNSs and (b) PdFe NCs.

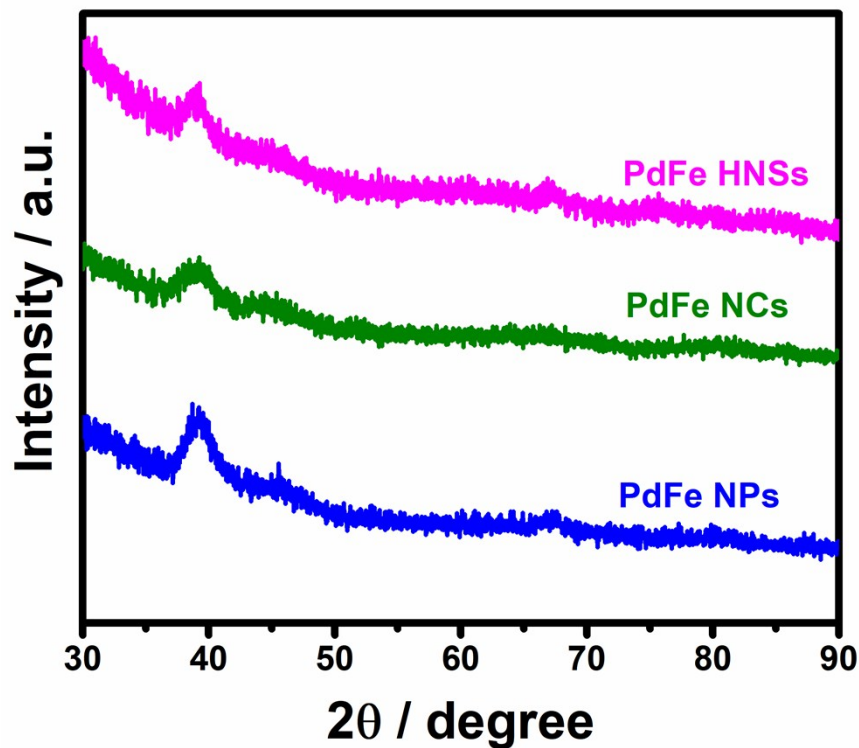


Fig.S6 XRD patterns of PdFe HNSs, PdFe NCs, and PdFe NPs.

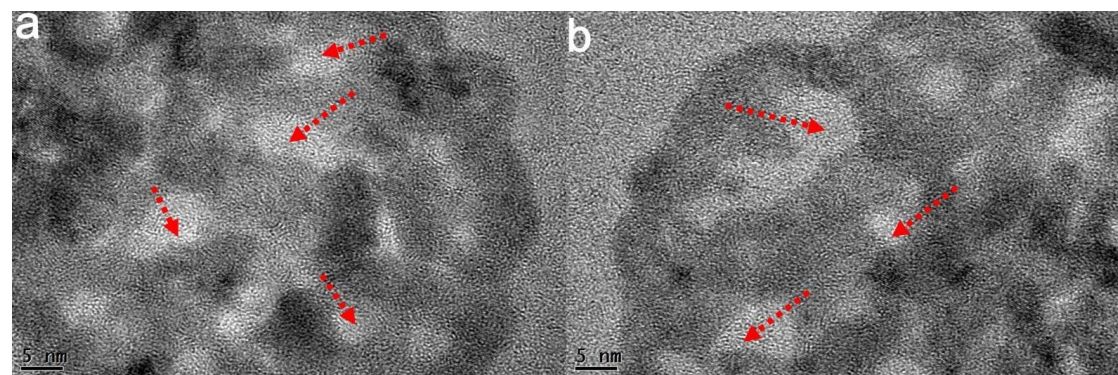


Fig.S7 Representative HRTEM images of PdFe NCs.

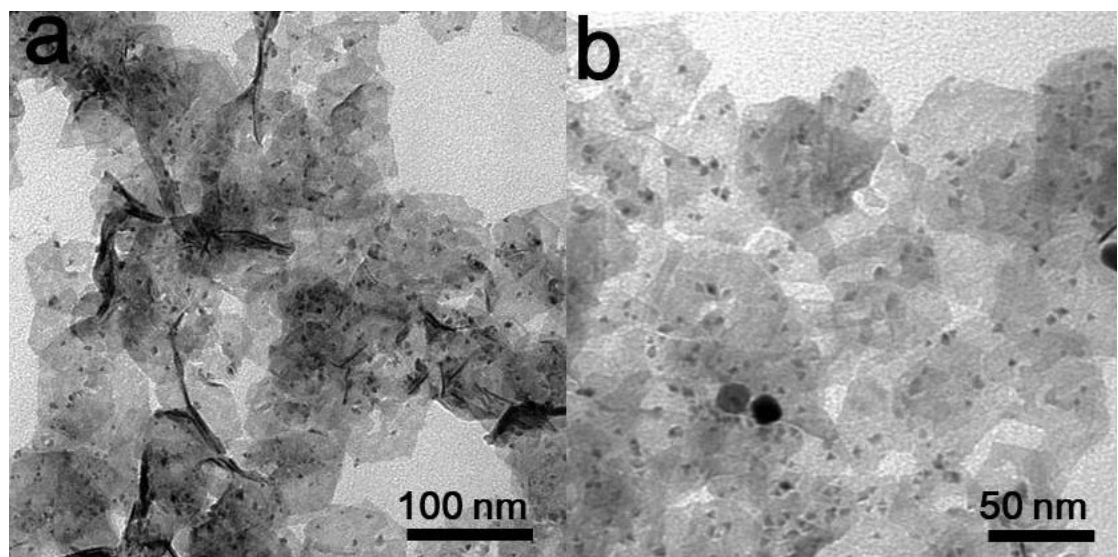


Fig.S8 TEM images of Pd NPs with different magnifications.

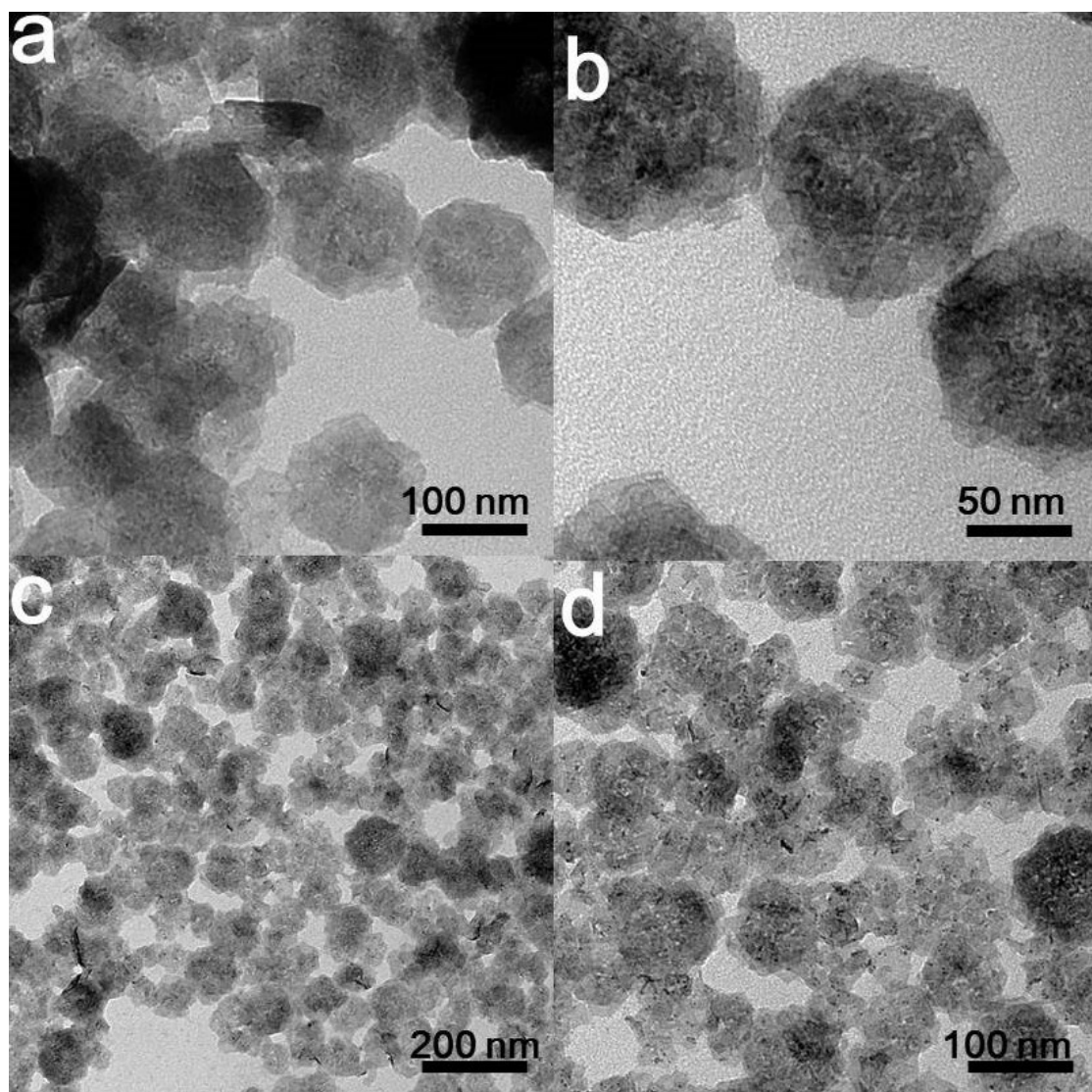


Fig.S9 TEM images of PdFe nanocrystals prepared under the same method of PdFe NCs while changing the $\text{Fe}(\text{Ac})_2$ into (a and b) $\text{Fe}(\text{acac})_2$ and (c and d) FeCl_3 with different magnifications.

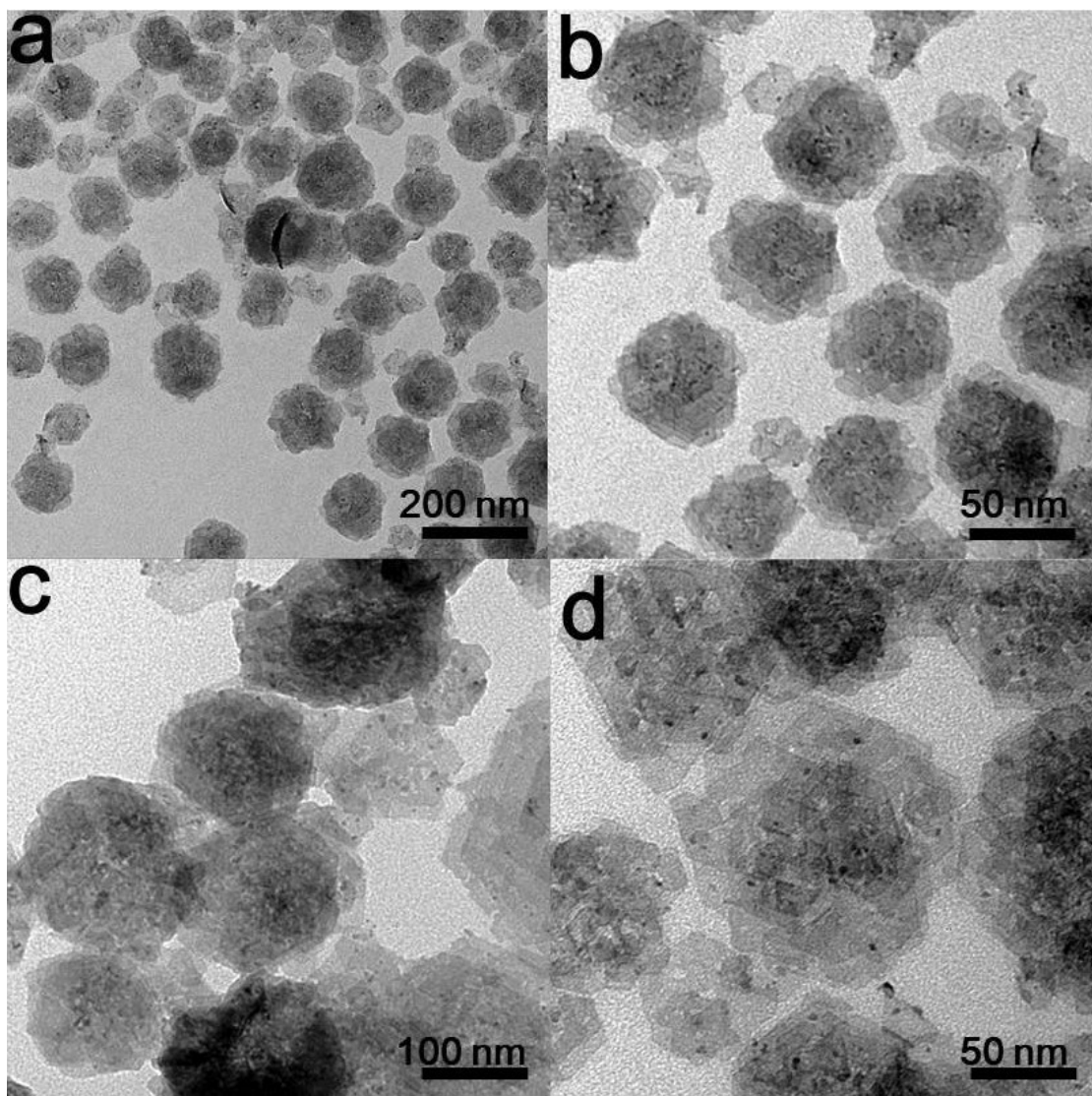


Fig.S10 TEM images of PdFe nanocrystals prepared under the same method of PdFe NCs while changing the Na_2PdCl_4 into (a and b) $\text{Pd}(\text{acac})_2$ and (c and d) K_2PdCl_4 with different magnifications.

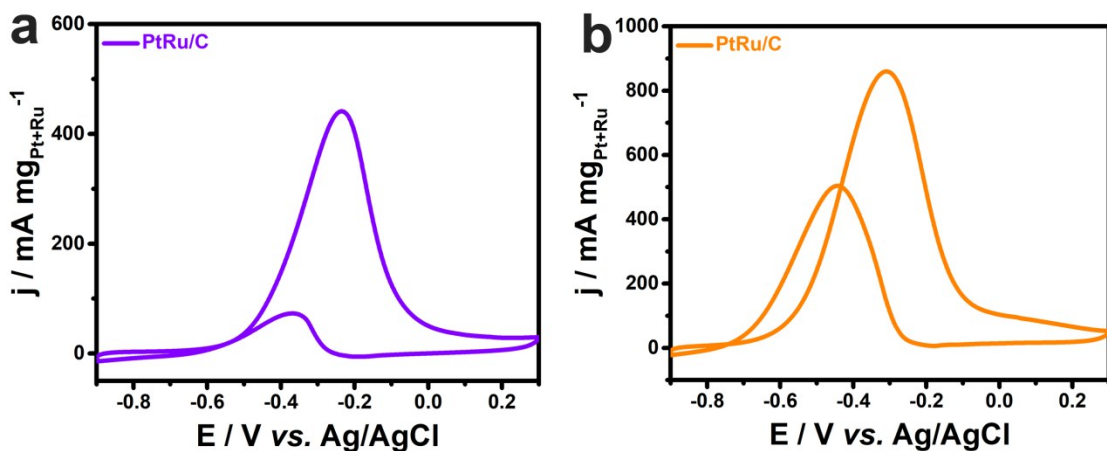


Fig.S11 CV curves of commercial PtRu/C catalyst in (a) 1 M KOH + 1 M CH₃OH solution and (b) 1 M KOH + 1 M CH₃CH₂OH at the scan rate of 50 mV s⁻¹.

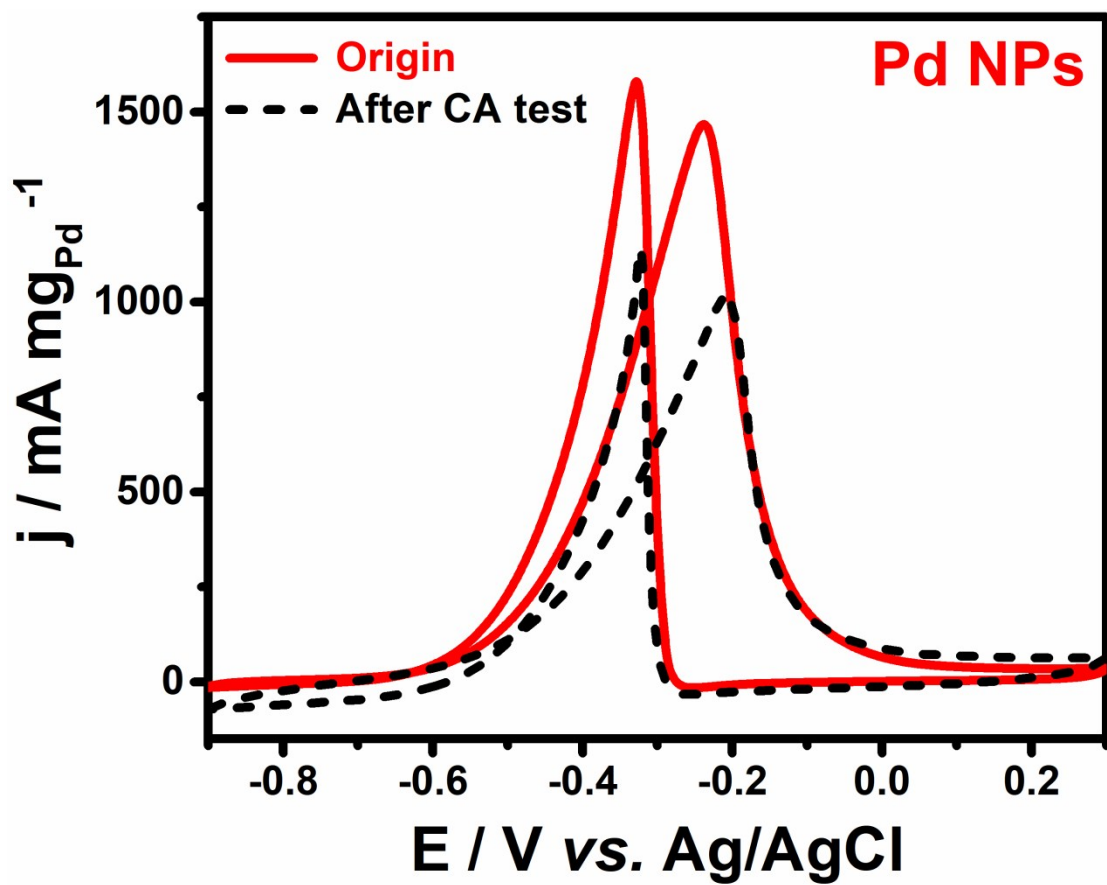


Fig.S12 CV curves of Pd NPs before and after CA test.

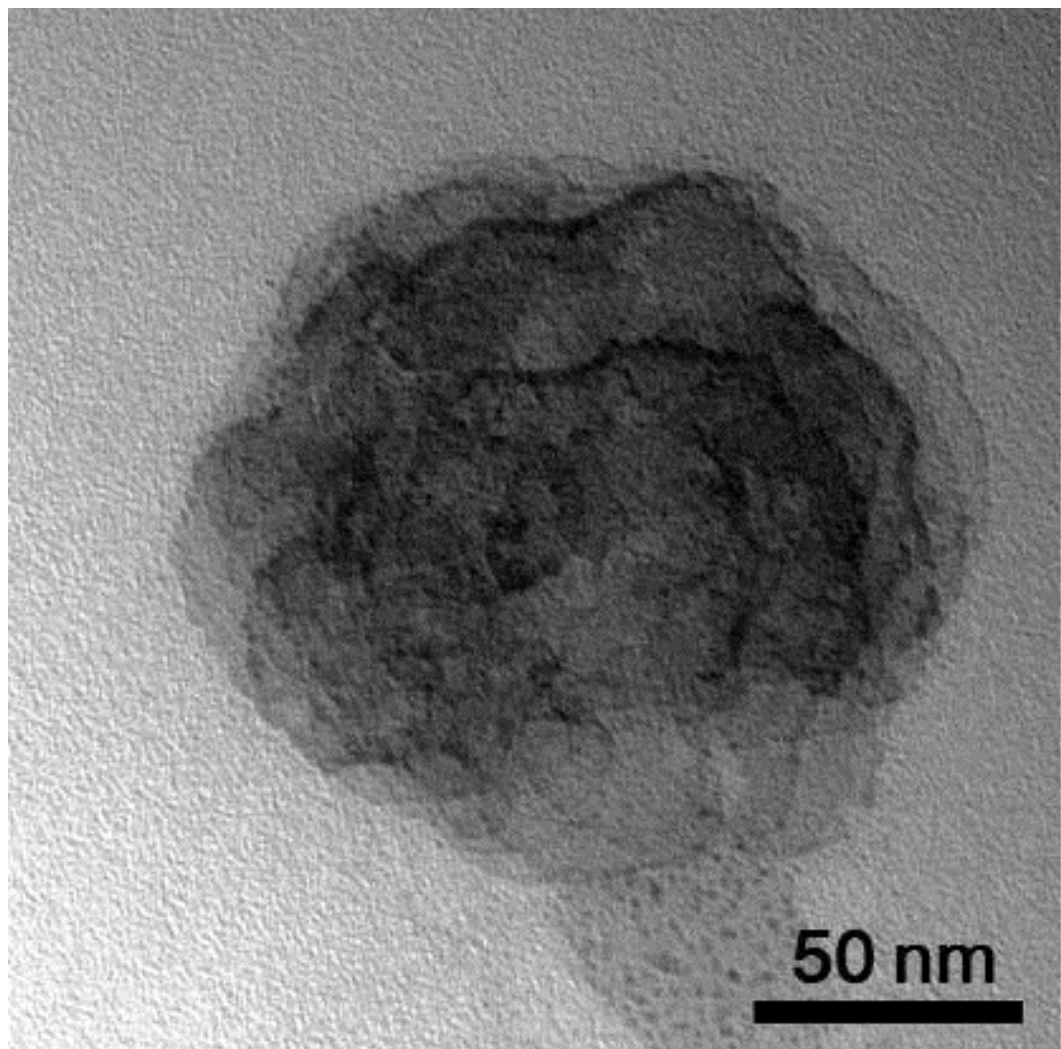


Fig.S13 TEM image of PdFe NCs after electrochemical tests.

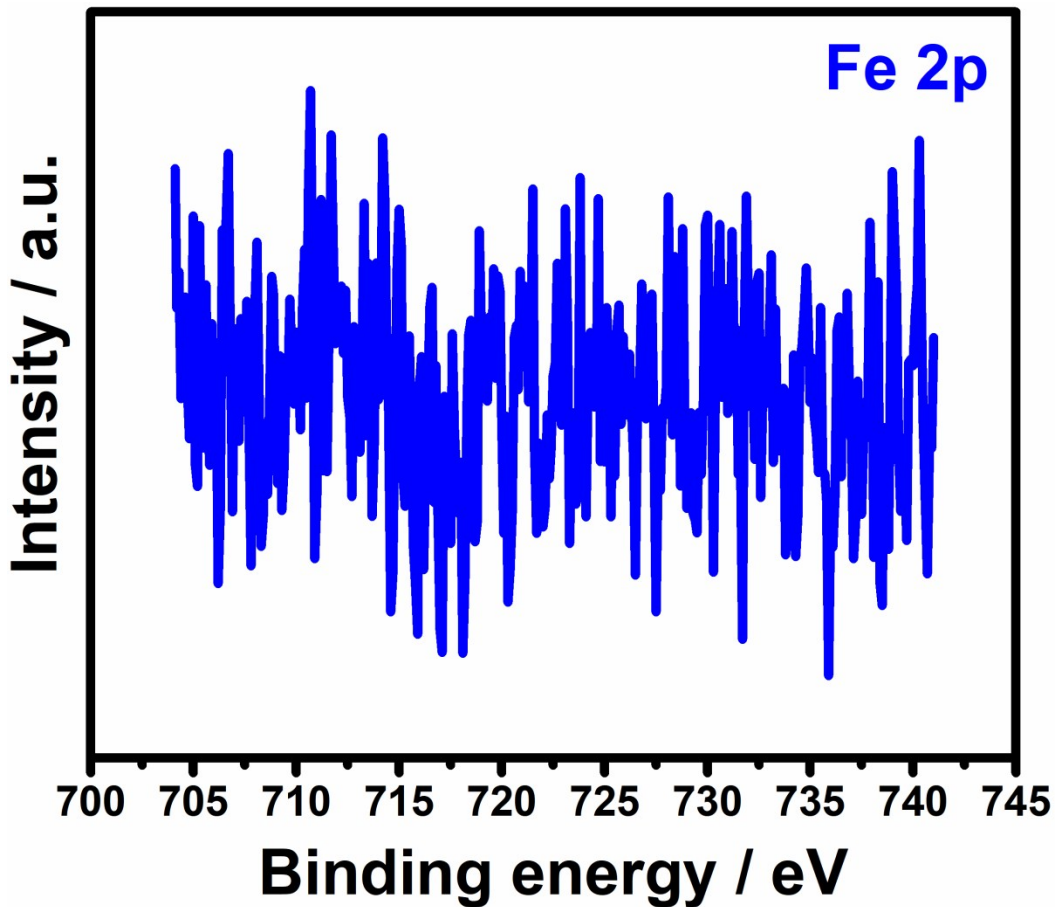


Fig.S14 High-resolution XPS spectrum of Fe 2p in PdFe NCs.

Table S1 MOR electrocatalytic activity comparison of PdFe NCs with recently reported catalysts

Catalysts	Peaks currents from CV curves		Electrolyte	References
	J_m (A/mg _{Pd})	J_s (mA/cm ²)		
PdFe NCs	1.07	3.4	1.0 M KOH + 1.0 M CH₃OH	This work
Pd ₂ Cu ₂ /rGO	0.90		1 M KOH + 1 M CH ₃ OH	1
PdNi/RGO	0.80		0.5 M KOH + 1 M CH ₃ OH	2
Pd/P	0.844		1 M KOH + 1 M CH ₃ OH	3
Pd ₃ Ru/C	1.04		0.5 M KOH + 1 M CH ₃ OH	4
PdCuCo/RGO	1.06	~ 0.92	1 M KOH + 1 M CH ₃ OH	5
Pd NFs/PPy@MWCNT S	0.725	1.69	0.5 M KOH + 1 M CH ₃ OH	6
Pt-TiO ₂ /ITO		1.8	1 M KOH + 1 M methanol	7
Pt ₃ Cu/C	~ 0.70	~ 0.50	0.5 M HClO ₄ + 1 M methanol	8

Table S2 EOR electrocatalytic activity comparison of PdFe NCs with recently reported catalysts

Catalysts	Peaks currents from CV curves		Electrolyte	References
	J_m (A/mg _{Pd})	J_s (mA/cm ²)		
PdFe NCs	2.6	8.3	1.0 M KOH + 1.0 M CH₃CH₂OH	This work
PdAg HNFs	~ 1.6		1.0 M KOH + 1.0 M CH ₃ CH ₂ OH	9
Pd/Ni(OH) ₂ /Ni	0.77		1.0 M KOH + 1.0 M CH ₃ CH ₂ OH	10
PdSn	1.3		1.0 M KOH + 1.0 M CH ₃ CH ₂ OH	11
PdNi	1.5		1.0 M KOH + 1.0 M CH ₃ CH ₂ OH	12
Au–Pd@Pd CSNFs	2.07		1.0 M KOH + 1.0 M CH ₃ CH ₂ OH	13
Pd NPs/CoP NSs	1.41	3.5	1.0 M KOH + 1.0 M CH ₃ CH ₂ OH	14
PdRu	1.15		1.0 M KOH + 1.0 M CH ₃ CH ₂ OH	15
Pd/PANI/Pd	0.35		1.0 M NaOH + 1.0 M CH ₃ CH ₂ OH	16

References

1. H. Ye, Y. Li, J. Chen, J. Sheng, X.-Z Fu, R. Sun, C.-P Wong, *J. Mater. Sci.* 2018, 53, 15871-15881.
2. J. Hu, X. Wu, Q. Zhang, M. Gao, H. Qiu, K. Huang, S. Feng, T. Wang, Y. Yang, Z. Liu, B. Zhao, *Langmuir* 2018, 34, 2685–2691.
3. k. Zhang, C. Wang, D. Bin, J. Wang, B. Yan, Y. Shiraishi, Y. Du, *Catal. Sci. Technol.*, 2016, 6, 6441-6447
4. T. Jurzinsky, P. Kammerer, C. Cremers, K. Pinkwart, J. Tübke, *J. Power Sources*, 2016, 303, 182-193.
5. F. Yang, B. Zhang, S. Dong, C. Wang, A. Feng, X. Fan, Y. Li, *J. Energy Chem.* 2019, 29, 72-78.
6. L.A. Fard, R. Ojani, J.B. Raoof, *Int. J. Hydrogen Energy*, 2016, 41, 17987-17994.
7. H. Zhang, W. Zhou, Y. Du, P. Yang, C. Wang, J. Xu, *Int. J. Hydrogen Energy*, 2010, 35, 13290-13297.
8. Y. Zhang, Z. Cui, Y. Zhang, D. He, X. Yan, Y. Bi, Y. Li, Z. Li, X. Sun, *ACS Appl. Mater. Interfaces* 2014, 6, 20, 17748-17752.
9. D. Bin, B. Yang, K. Zhang, C. Wang, J. Wang, J. Zhong, Y. Feng, J. Guo, Y. Du, *Chem. Eur. J.* 2016, 22, 16642-16647.
10. C. Li, H. Wen, P.-P Tang, X.-P. Wen, L.-S.Wu, H.-B. Dai, P. Wang, *ACS Appl. Energy Mater.* 2018, 1, 11, 6040-6046.
11. A. Zalineeva, A. Serov, M. Padilla, U. Martinez, K. Artyushkova, S. Baranton, C. Coutanceau, P. Atanassov, *Electrochim. Commun.* 2015, 57, 48-51.
12. Y. Feng, D. Bin, B. Yan, Y. Du, T. Majima, W. Zhou, *J. Colloid Interface Sci.* 2017, 493, 190-197.
13. X. Qiu, Y. Dai, Y .Tang, T. Lu, S. Wei, Y. Chen, *J. Power Sources*, 2015, 278, 430-435.
14. S.-H. Ye, J.-X. Feng, G.-R. Li, *ACS Catal.* 2016, 6, 11, 7962-7969
15. K. Zhang, D. Bin, B. Yang, C. Wang, F. Ren, Y. Du, *Nanoscale* 2015, 7, 12445-12451.
16. A.-L. Wang, H. Xu, J.-X. Feng, L.-X. Ding, Y.-X. Tong, G.-R. Li, *J. Am. Chem. Soc.* 2013, 135, 10703-10709.